Hindawi
Advances in Civil Engineering
Volume 2021, Article ID 8811303, 11 pages
https://doi.org/10.1155/2021/8811303

Research Article

Dynamic Characteristics of Lightweight Aggregate Self-Compacting Concrete by Impact Resonance Method

Ning Li[1], **Sisi Zhang**[2], **Guangcheng Long**[3], **Zuquan Jin**[1], **Yong Yu**[1], **Xiaoying Zhang**[1], **Chuansheng Xiong**[1] and **He Li**[4]

[1]*Engineering Research Center of Concrete Technology in Marine Environment, Ministry of Education, Qingdao University of Technology, Qingdao 266033, China*
[2]*Institute of Concrete Construction, Leibniz University Hannover, Hannover 30167, Germany*
[3]*School of Civil Engineering, Central South University, Changsha 410075, China*
[4]*College of Mechanical and Electronic Engineering, Shandong University of Science and Technology, Qingdao 266590, China*

Correspondence should be addressed to Guangcheng Long; longguangcheng@csu.edu.cn, Xiaoying Zhang; zhangxy@qut.edu.cn, and He Li; lihe_hit@163.com

Received 20 June 2020; Revised 25 January 2021; Accepted 6 March 2021; Published 27 March 2021

Academic Editor: Melina Bosco

Understanding the dynamic behavior of Lightweight Aggregate Self-Compacting Concrete (LWASCC) is of importance to the safety of concrete structures serving in dynamic loading conditions. In this study, the fundamental dynamic properties of LWASCC with three types of LWA were investigated by the impact resonance method. Results show that the dynamic elastic and shear modulus generally decrease with the increase of LWA volume fraction, whereas three types of LWA exert limited influence on dynamic Poisson's ratio. The dynamic elastic and shear modulus show good linear dependence upon compressive strength. The inclusion of three types of LWA significantly increases the damping ratio, indicating significantly enhanced damping capacity of LWASCC under dynamic loading conditions. The damping ratio of LWASCC is improved by 2.0%, 4.4%, and 2.9% when adding 1% (by volume) expanded clay, rubber, and expanded polystyrene, respectively. The compressive strength and dynamic performances of LWASCC are highly influenced by the intrinsic properties (elastic modulus, damping capacity, wettability, etc.) and geometrical characteristics (size, surface roughness, etc.) of LWA, as well as the LWA-matrix bonding capacity.

1. Introduction

Self-compacting concrete (SCC) is a special type of high-performance concrete developed over the last few decades, which consolidates under its own weight instead of mechanical vibration and has excellent flowability, segregation resistance, filling, and passing ability in the fresh state [1]. These advantages enable SCC to be successfully used in confined areas and densely reinforcement elements [2–4]. However, SCC still has some disadvantages such as high brittle characteristics and high density, which would limit its broader application in civil engineering [5]. A possible solution to the problem is to partially or totally substitute natural aggregate with lightweight aggregate (LWA) to produce lightweight aggregate self-compacting concrete (LWASCC) [6–9]. LWA can be divided into several types according to its source including natural LWA (pumice, volcanic cinder, etc.), artificial LWA (expanded polystyrene beads, expanded clay ceramsite, etc.), and industrial waste LWA (rubber particles, coal cinder, etc.). LWASCC combines the advantages of both SCC and LWA concrete, having the promising application prospect in long-span bridges and high-rise buildings as well as reducing the dimensions of elements [10, 11].

However, the incorporation of LWA leads to a non-negligible strength loss of concrete as a result of the low elastic modulus and strength of the LWA compared with the other components in concrete [12]. The strength loss was also observed when expanded clay [13], expanded shale [14], perlite [15], pumice [16, 17], and expanded polystyrene

beads [18] were included in concrete. In some cases, the extra vibration in the preparing process of concrete may result in the upward movement of LWA and thus increased segregation tendency [19, 20]. The self-compacting technology can effectively reduce these problems within adequate workability, due to the absence of vibration and this would alleviate the remarkable strength loss. In addition, some cementitious materials, such as silica fume and fly ash used in SCC, can successfully enhance the weak interfaces between LWA and cement matrix [21]. Long et al. [22] conducted a wide range of literature research on rubber concrete and summarized that adding 1.0% (by volume) rubber particles resulted in a 4.6% reduction in compressive strength of normal concrete, which was slightly higher than that of SCC (4.1%). They attributed the greater strength loss of normal concrete to the poorly developed rubber-hardened cement paste interface induced by vibration in the preparing process.

With the increasing complexity of the service environment in the field of civil engineering, many concrete structures have been subjected to occasional or frequent dynamic loads, such as railway track structures undergoing vibration of a high-speed train, offshore structures suffering from repeated sea wave impact, protective structures exposed to bomb blast, and civil architectures at the risk of earthquakes in seismic areas [23]. Previous research on normal LWA concrete has revealed that the use of LWA as alternatives to natural aggregate can present some promising performances under these conditions. Zheng et al. [24] investigated the dynamic properties of rubberized concrete using a free vibration method and observed that the damping ratios of rubberized concrete improved considerably compared to those of normal concrete. They also highlighted that the rubber size, type, and content played an important role in affecting the damping property of rubberized concrete. Nikbin and Golshekan [25] also experimentally investigated the lightweight concrete with expanded polystyrene (EPS) and found that the ultrasonic waves velocity of concrete decreased with the increase of EPS volume fraction. They classified EPS concretes as good in terms of quality according to the BIS classification for the quality of the concrete based on the velocity of ultrasonic waves. Long et al. [26] further investigated the dynamic mechanical properties of steam-cured concrete and observed enhanced damping ratio when expanded clay ceramsite or ceramsite sand was incorporated. They attributed the enhanced dynamic properties of concrete to the porous characteristics of LWA and excess free water stored inside it.

The existing research on LWASCC mainly focuses on its fresh properties and basic static mechanical properties [27–30]. Nevertheless, there is still insufficient experimental data relating to how LWA type and content affect the dynamic characteristics of LWASCC. The dynamic response of SCC with LWA is of great importance to the safety of concrete structures serving in dynamic loading conditions. Understanding the dynamic properties of concrete can significantly improve the structural reliability when subjected to dynamic loads. Therefore, in this study, the fundamental dynamic characteristics of LWASCC with three typical types of LWA at incremental volume percentages were comparatively investigated by the impact resonance method. The objective of this study is to help understand the dynamic behavior of LWASCC, develop LWASCC with anticipated dynamic properties, and facilitate its potential applications.

2. Materials and Methods

2.1. Materials. The cementitious materials include P·O 42.5 cement, fly ash, silica fume, and hydroxypropyl methylcellulose (HPMC). HPMC is used as the viscosity-modifying material with a viscosity of 20 000 Pa·s. The chemical composition and physical properties of cement, fly ash, and silica fume are tabulated in Table 1 and the corresponding particle distributions are shown in Figure 1(a).

Five types of aggregate including two natural aggregate and three LWA are used in this study. Locally available river sand is used as natural fine aggregate with a fineness modulus of 2.6 and an apparent density of 2650 kg/m^3. Crushed gravel is used as natural coarse aggregate with an apparent density of 2670 kg/m^3. Grinded waste tire rubber (*R*) particles and commercially available expanded polystyrene (EPS) beads are used as LWA to substitute natural fine aggregate. Expanded clay (EC) ceramsite is used as alternative LWA of natural coarse aggregate. The physical properties of three types of LWA are listed in Table 2 and the particle distribution of all types of aggregates is shown in Figure 1(b).

The superplasticizer (SP) used in this study is polycarboxylate-based and it has a density of 1050 kg/m^3 and a water-reducing rate of 26%. The mixing water is tap water.

2.2. Mix Proportion. The mix proportions designed in this study are as follows: in Series I, the control SCC was designed with a total cementitious material (also named as binder) content of 490 kg/m^3 and a water-binder ratio (by mass) of 0.38. In addition, HPMC was introduced with a content of 0.15 kg/m^3, aiming at increasing the viscosity of the fresh mixture and reducing the segregation risk caused by LWA. The mix proportion of control SCC is listed in Table 3 in detail. In Series II (named SCC-EC), the natural coarse aggregate was substituted by EC at levels of 10%, 20%, 30%, 40%, 50%, and 60% by volume, respectively. In Series III (named SCC-R) and IV (named SCC-EPS), the natural fine aggregate was substituted by *R* and EPS at levels of 5%, 10%, 15%, 20%, 25%, and 30%, respectively. In each series, SP was used in quantities of 1.0% (by mass of cementitious materials), for the purpose of maintaining proper workability of fresh SCC.

2.3. Mixing Procedure and Specimen Preparation. The mixing procedure and specimen preparation of LWASCC were performed as follows: the dry materials including cementitious materials and aggregate were firstly blended in a 60 L mixer at a speed of 50 r/min for 30 seconds. Then, the SP-water solution (mixed beforehand) was added and all the materials were mixed for 3 more minutes. After the

Table 1: Physical and chemical properties of cementitious materials.

Type	Cement	Fly ash	Silica fume
Chemical properties (wt. %)			
SiO_2	24.6	52.3	90.6
Al_2O_3	7.30	26.3	0.60
Fe_2O_3	4.00	9.70	1.50
CaO	59.7	3.70	0.30
MgO	3.80	1.20	0.60
SO_3	2.50	0.20	1.30
eq-Na_2O	0.60	1.80	—
Loss on ignition	2.20	4.50	1.80
Physical properties			
Specific gravity	3.10	2.31	2.10
Specific surface area (m^2/kg)	350	460	17800

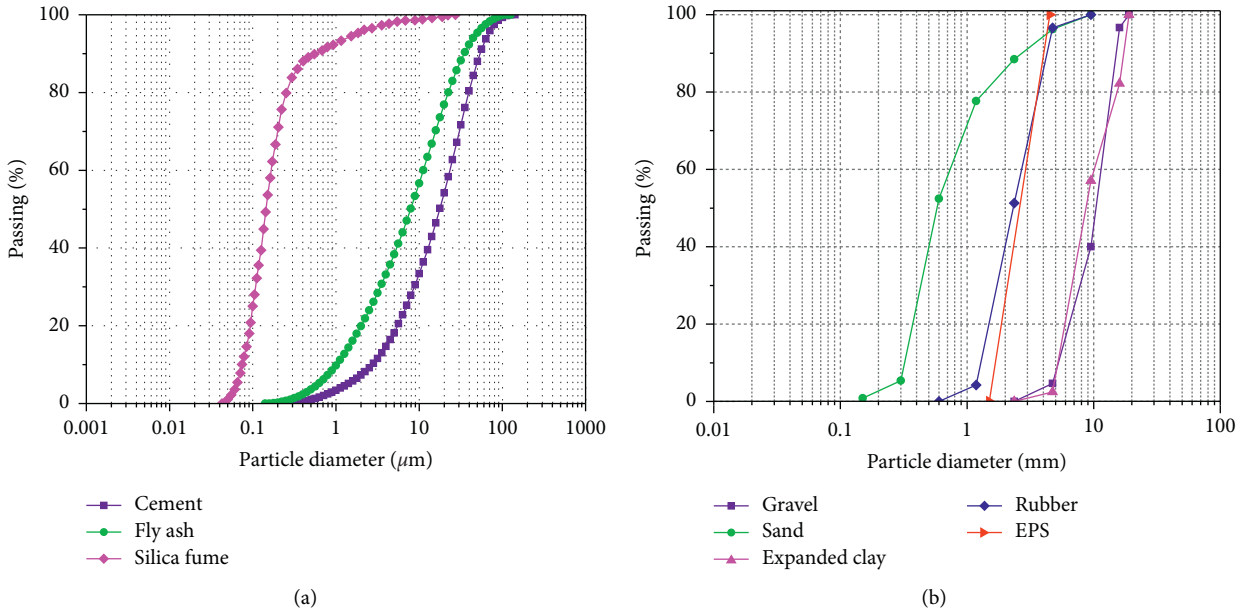

Figure 1: The particle distribution of raw materials. (a) Cementitious materials. (b) Aggregates.

Table 2: Physical properties of LWA.

Properties	EC	*R*	EPS
Apparent density (kg/m^3)	820	1000	10
Elastic modulus (MPa)	—	3.4	0.4
Cylindrical compressive strength (MPa)	2.8	—	—
Water absorption (wt. %)	13.3	<1.0	<1.0
Size distribution (mm)	4.75–15.0	1.2–4.0	1.5–4.5

workability of fresh LWASCC was tested, the mixture was cast into 100 mm × 100 mm × 100 mm cubic molds (for compression test) and 100 mm × 100 mm × 300 mm cuboid molds (for the dynamic test) to form specimens. The ambient temperature was around 20°C–25°C. The specimens were demolded after one day and then cured in a standard curing room till 28 days. The standard curing room had a temperature of (20 ± 2) °C and a relative humidity over 95%.

Table 3: Mix proportions of control SCC (kg/m^3).

Cement	Fly ash	Silica fume	HPMC	Sand	Gravel	Water	SP
343	123	24	0.15	795	898	185	4.9

2.4. Testing Method

2.4.1. Workability Test. SCC is characterized by its excellent workability in the fresh state including both flowability and passing ability. The incorporation of LWA would inevitably make a difference to the workability of SCC. Therefore, in this study, slump-flow test and J-ring test were conducted to evaluate the workability of LWASCC in accordance with ASTM C 1611 [31] and 1621 [32]. In the slump-flow test, slump-flow value (the final flow diameter) and T_{50} (the time to reach a 50 cm diameter) were measured to evaluate the flowability of fresh LWASCC. In the J-ring test, the passing ability is determined by the difference of slump flow and J-ring flow.

2.4.2. Compressive Strength Test. The compressive strength test was conducted with a universal material testing machine according to Chinese standard GB/T 50081 [33]. The loading rate was kept at 0.15 mm/min. Three 100 mm × 100 mm × 100 mm cubic specimens were measured for each group.

2.4.3. Dynamic Test. In this study, an Emodumeter testing system was employed to measure the dynamic modulus of 100 mm × 100 mm × 300 mm cuboid specimens by impact resonance method according to ASTM C 215 [34], as shown in Figure 2. Three specimen replicates were performed for each testing method. The value of dynamic elastic modulus (E_d) and dynamic shear modulus (G_d) were automatically calculated by the testing system according to the following equations:

$$E_d = DM\ \left(n'\right)^2, \tag{1}$$

$$G_d = BM\left(n''\right)^2, \tag{2}$$

where D and B are two parameters related to the dimension of specimens; M is the mass of specimens; n' is fundamental longitudinal frequency; and n'' is fundamental torsional frequency. Then, the dynamic Poisson's ratio (μ_d) can be calculated according to

$$\mu_d = \frac{E_d}{\left(2G_d\right) - 1}. \tag{3}$$

Figure 3 shows the acceleration attenuation curve provided by the testing system. According to [26], the damping ratio (ζ) of the specimen can be calculated by

$$\zeta = \frac{1}{2\pi n} \ln \frac{A_i}{A_{i+n}}, \tag{4}$$

where A_i and A_{i+n} are the acceleration peak values at the first cycle and $(i+n)$ th cycle after impact on the specimen, respectively.

3. Results and Discussion

3.1. Workability. For the purpose of comparison, in the following sections, the content of each type of LWA is changed into its volume fraction per cubic meter concrete. Figure 4 shows the workability of LWASCC with three types of LWA. For Series I, the control SCC mixture has a slump flow of 690 mm and a slump-flow time (T_{50}) of 3.5 s. The difference between slump flow and J-ring flow is 18 mm. As shown in Figures 4(a) and 4(b), increasing EC content generally results in a slight increase in slump flow and a decrease in T_{50}. In addition, the difference between slump flow and J-ring flow decreases with increasing EC content, as shown in Figure 4(c). As suggested by ASTM C 1621 [32], fresh LWASCC with a difference value of 0–25 mm can be classified as "no visible blocking." This indicates that the addition of EC improves the workability of LWASCC in terms of both flowability and passing ability, whereas, for R and EPS, opposite tendencies were observed. The inclusion of R and EPS leads to a remarkable reduction in flowability of LWASCC, as shown in Figures 4(a) and 4(b). In addition, it can be observed from Figure 4(c) that the difference between slump flow and J-ring flow increases with R or EPS content. It should be noted that varying the volume fraction of R and EPS from 4.5% to 9.0% leads to a different value of 25 mm–50 mm, implying "minimal to noticeable blocking" according to ASTM C1621 [32].

The workability variations of LWASCC are highly related to the physical properties (density, geometrical shape, etc.) of LWA and its interaction with other particles in the mixture. For LWASCC with EC aggregate, the workability of the fresh mixture is a counteraction of density and geometrical shape of EC. On one hand, the addition of low-density EC reduces the self-weight of LWASCC, which decreases the plastic deformability of fresh LWASCC under its own weight. On the other hand, as can be seen from Figure 1(b), the spherical or ellipsoid shape of EC can effectively reduce its friction with other particles in the flowing process and thus increase the workability of the mixture. The combined effect of the two mechanisms results in a slightly improved workability of fresh LWASCC, as provided in Figure 4, whereas for LWASCC with R and EPS, the poor workability is dominated by the low density of LWA. In addition, the high surface roughness of rubber increases the interparticle friction, resulting in reduced flowability and passing ability [35, 36], while for EPS, the extremely low elastic modulus (as shown in Table 2) makes it very easy to undergo large deformation and thus the shape effect disappears.

3.2. Compressive Strength. Figure 5(a) shows the 28-day compressive strength (f_c) results of LWASCC with three types of LWA. The compressive strength of control SCC is 31.7 MPa. As expected, the inclusion of LWA generally leads to a decrease in compressive strength. Specifically, varying the R and EPS volume fraction from 0.5% to 9.0% reduces the 28-day compressive strength of SCC by 10.7%–29.0% and 5.7%–27.8%, respectively, whereas, for LWASCC with EC, increasing EC volume fraction from 3.4% to 20.2% results in a 7.6%–36.3% reduction in compressive strength.

Figure 5(b) further gives the reduction rate of compressive strength with volume fractions of LWA. The corresponding linear fitting formulas and correlation coefficients are also provided. As shown in Figure 5(b), the compressive strength of LWASCC shows very similar tendency with increasing R and EPS amount. The compressive strength of LWASCC is reduced by 3.9% and 4.0% when adding 1% R and EPS, respectively, which is twice as large as that of EC (2.0%). This indicates that the reduction effect of EC on the compressive strength of LWASCC is much lower than that of R and EPS. This may result from the much denser ITZ of EC-matrix than those of the other LWA-matrix. The corresponding evidence will be provided in the following sections.

3.3. Dynamic Elastic Modulus. The dynamic elastic modulus is an index to evaluate the elastic deformation capacity before the development of microcracks under dynamic

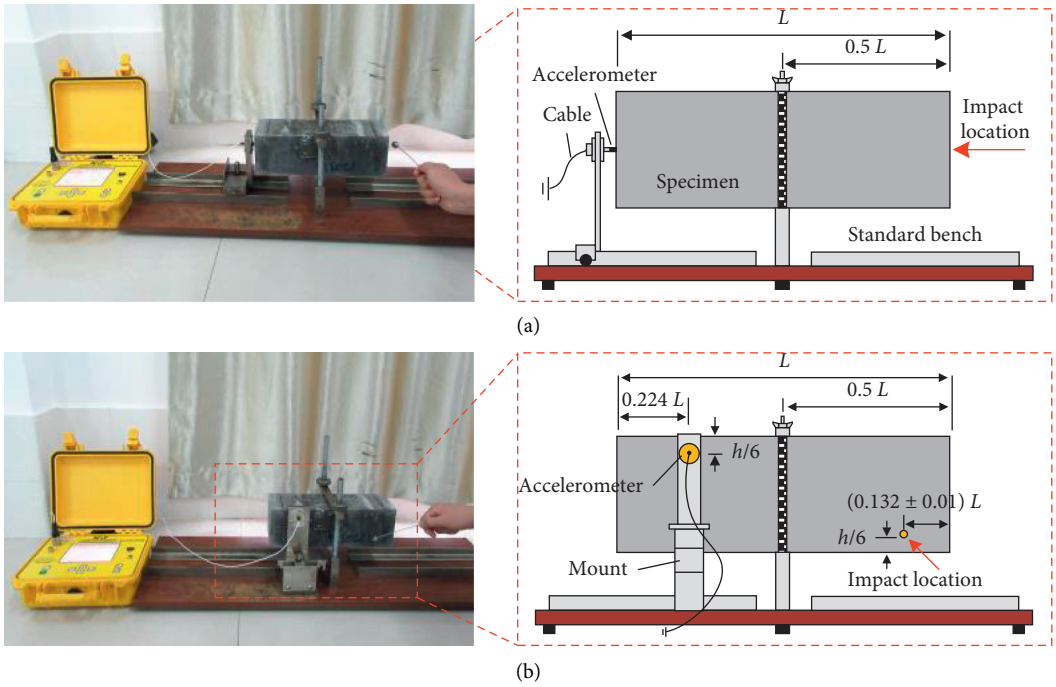

Figure 2: Dynamic test. (a) Dynamic elastic modulus. (b) Dynamic shear modulus.

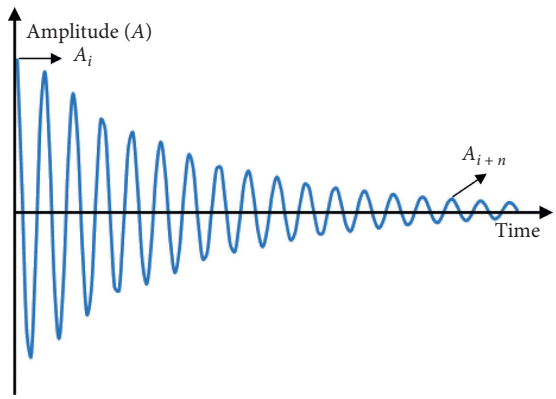

Figure 3: The acceleration attenuation curve.

loads. The dynamic elastic modulus measured by the non-destructive testing method is often used for stress analysis of structures subjected to earthquake or impact loading. It is reported that the value of dynamic elastic modulus is highly influenced by aggregate type and quantity [37].

Figure 6 provides the 28-day dynamic elastic modulus of LWASCC with three types of LWAs. The dynamic elastic modulus of SCC is 36.9 GPa when no LWA is introduced. It can be observed from Figure 6 that increasing LWA volume fraction generally results in a reduction in dynamic elastic modulus, and this is in line with the tendency of compressive strength, as shown in Figure 5(a).

In order to describe the influence of LWA on dynamic elastic modulus more accurately, Figure 6(b) further gives the relationship between the reduction rate of dynamic elastic modulus and volume fraction of three types of LWAs. The corresponding fitting formulas and correlation coefficients are also provided. As can be observed from Figure 6(b), the reduction rate of dynamic elastic modulus shows good linear dependence on the volume fraction of LWA. Increasing 1% volume of EC, *R* and EPS reduce the dynamic elastic modulus of SCC 1.83%, 1.61%, and 2.30%, respectively.

3.4. Dynamic Shear Modulus. Dynamic shear modulus (G_d) is a parameter to evaluate the rigidity of concrete-like materials under dynamic loads. Figure 7(a) illustrates the 28-day dynamic shear modulus of LWASCC with three types of LWAs. The dynamic shear modulus of SCC is 14.7 GPa when no LWA is introduced. As shown in Figure 7(a), the dynamic shear modulus of SCC generally shows a decreasing trend as the LWAs volume fraction increases. Figure 7(b) further provides the relationship between the reduction rate of dynamic shear modulus and the volume fraction of LWA. The dynamic shear modulus of SCC is decreased by 1.88%, 1.51%, and 2.52% when the volume fraction of EC, *R*, and EPS is increased by 1%, respectively. This trend is very similar to the variations of dynamic elastic modulus, as shown in Figure 6(b).

3.5. Dynamic Poisson's Ratio. Dynamic Poisson's ratio (μ_d) is defined as the ratio of axial strain to transverse strain under dynamic loads, which is an elastic index to characterize the transverse deformation of concrete-like materials [38]. The value of dynamic Poisson's ratio is calculated based on dynamic elastic and shear modulus, as expressed in equation (1). Figure 8 illustrates the 28-day dynamic Poisson's ratio of SCC with three types of LWAs. The dynamic Poisson's ratio of control SCC is 0.26. The addition of *R* and EPS results in a

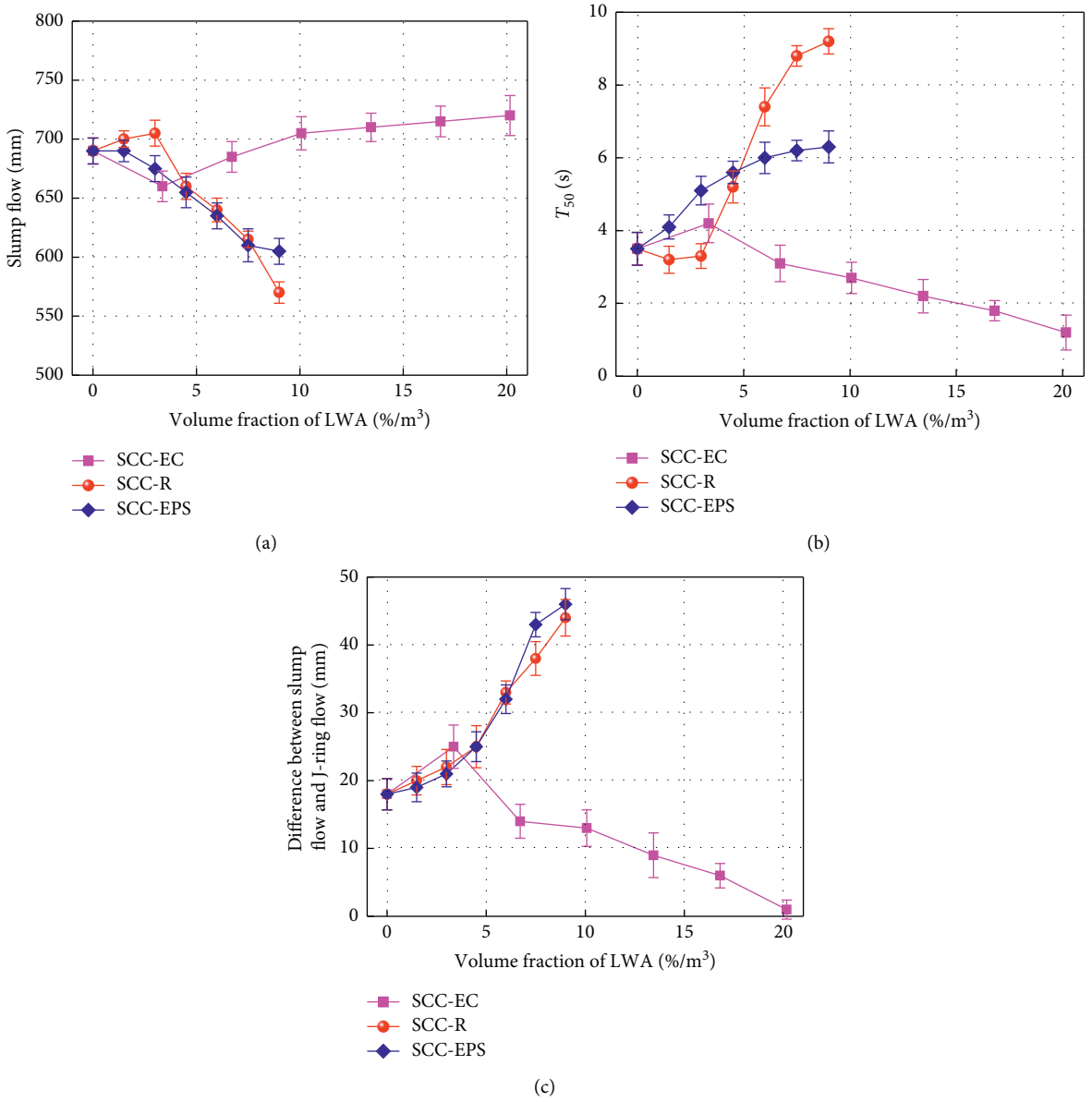

Figure 4: Workability of LWASCC. (a) Slump flow. (b) T_{50}. (c) Passing ability.

slight decrease and increase in dynamic Poisson's ratio, respectively, with a maximum amplitude of variation no more than 10%. In addition, the dynamic Poisson's ratio of LWASCC shows a fluctuant trend with increasing EC volume fraction. This indicates that the incorporation of LWA exerts a limited influence on the transverse deformation capacity of LWASCC when subjected to dynamic loads.

3.6. Damping Ratio. Damping is a very important dynamic characteristic of concrete-like materials, which is characterized by the dissipation of vibration energy. It can be used to evaluate the structure's dynamic response and identify structural damage [39]. Damping ratio (ζ) is one of the most frequently used parameters to characterize the damping properties of concrete-like materials under dynamic loads.

Figure 9(a) shows the 28-day damping ratio of LWASCC with three types of LWA. The damping ratio of SCC is 0.48 when no LWA is introduced, and the value is considerably promoted as the amount of LWA increase, which indicates that the addition of three types of LWA provides significantly enhanced energy dissipation capacity under dynamic loading conditions. The increase amplitude can reach up to 44.4%, 47.5%, and 28.3% when 20.2% EC, 9.0% *R*, and 9.0% EPS are introduced. Figure 9(b) further provides the increase rate of damping ratio of LWASCC with a volume fraction of LWA. It can be seen from Figure 9(b) that the damping ratio of SCC is improved by 2.0%, 4.4%, and 2.9% when the volume fraction of EC, *R*, and EPS is increased by 1%, respectively. It can be concluded that the addition of *R* provides SCC with the best damping properties. The outstanding damping performance makes it possible for LWASCC to be used in some occasions where vibration damping is required.

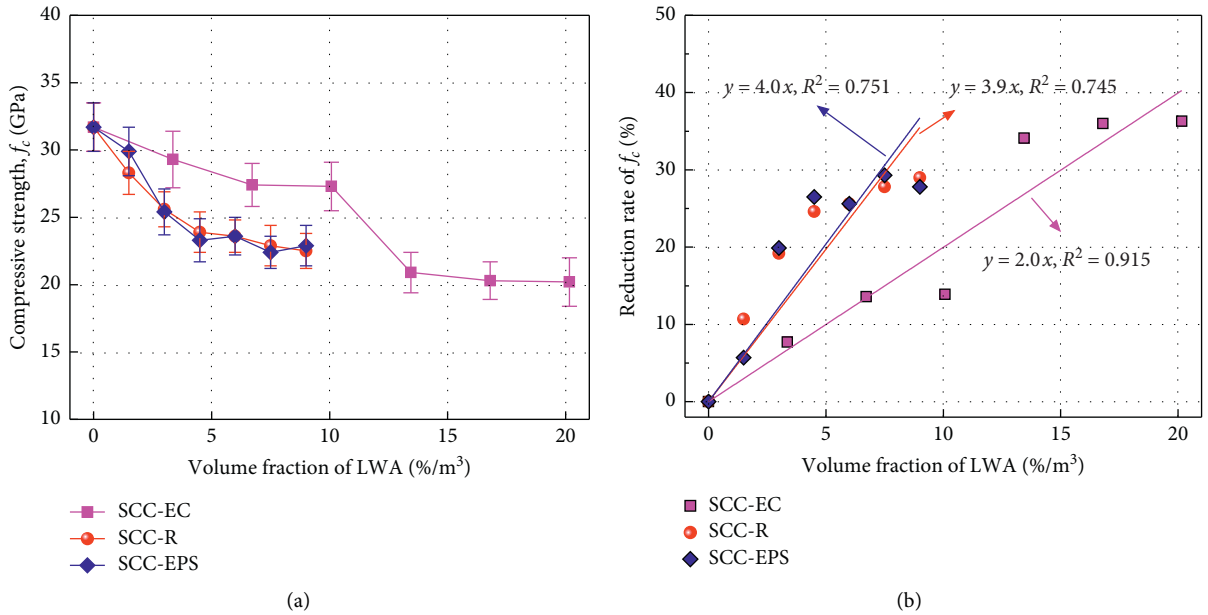

Figure 5: (a) Compressive strength and (b) its reduction rate of LWASCC.

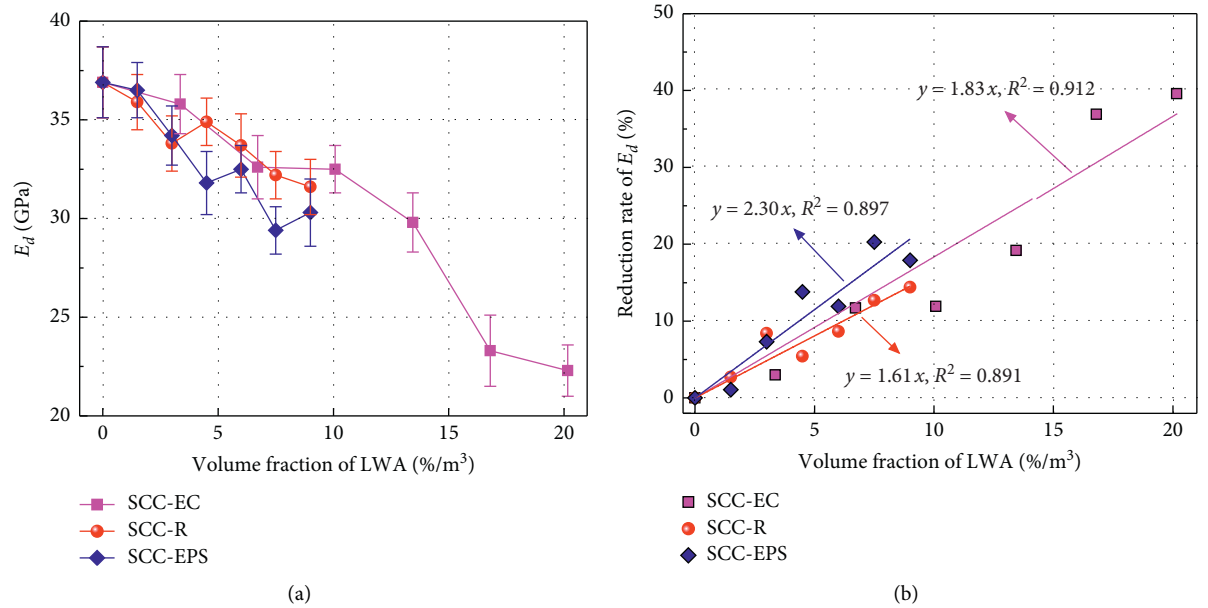

Figure 6: (a) E_d of LWASCC. (b) Reduction rate of E_d with LWAs.

4. Mechanisms

As discussed above, the introduction of expanded clay, rubber, and EPS exerts different influences on both static and dynamic characteristics of LWASCC, and the different performances of LWASCC are highly dependent upon the inherent properties of LWA itself and its interaction with other components in LWASCC. The detailed mechanisms are analyzed as follows.

Figure 10 illustrates the schematic diagram of SCC with different types of aggregates and Figure 11 shows the micrographs of the interfacial transition zone (ITZ) between aggregates and SCC matrix captured by an optical microscope. As shown in Figures 10(a) and 11(a), SCC is an aggregate-suspension system with all the aggregates uniformly dispersed in the cement matrix. In the preparation and hydration process of SCC, some microdefects including ITZs, microcracks, and pores are generated. When subjected

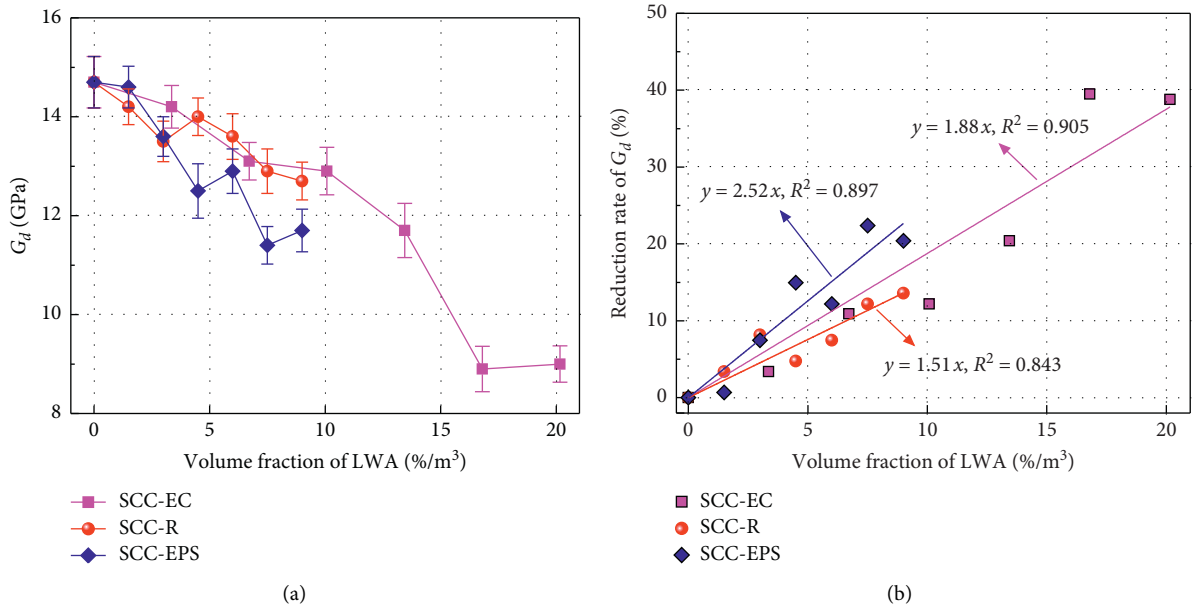

Figure 7: (a) G_d of LWASCC. (b) Reduction rate of G_d with LWAs.

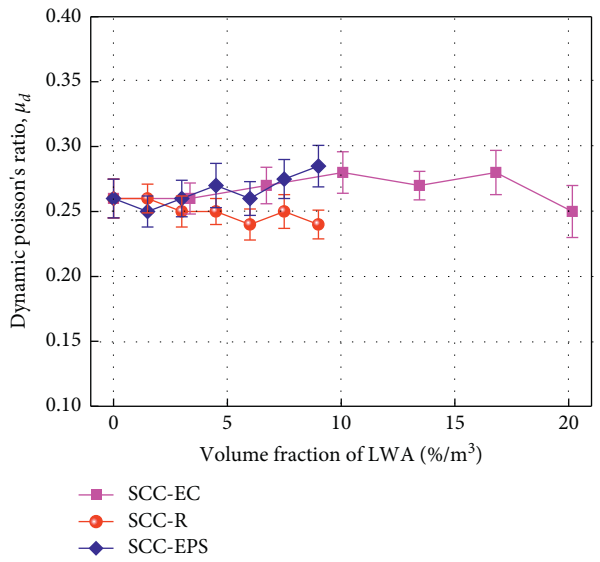

Figure 8: Dynamic Poisson's ratio of LWASCC.

to uniaxial compression loads, these microdefects propagate and finally interconnect to each other which causes the failure of concrete. Compared with natural aggregate, LWA typically has much lower mechanical strength and elastic modulus themselves. Therefore, the replacement of natural aggregate with LWA will inevitably result in the strength loss of SCC, as shown in Figure 5(a). As shown in Figure 10(b), the relatively higher water absorption capacity and porous structure make it easier for moisture exchange in EC-matrix interfaces [26], which enables a higher extent of cement hydration and consequently more compacted ITZ structures. This can be confirmed by the micrographs presented in Figure 11(b). For *R* and EPS, however, the hydrophobic nature of the particle surfaces leads to much poorly developed ITZs, as shown in Figures 10(c)–10(d) and observed in Figures 11(c)–11(d). In addition, the elastic modulus of *R* and EPS is one or two order of magnitudes lower than that of the SCC matrix, leading to the specimens easier to fail during the loading process. The above behaviors can be used to explain the reason why the reduction effect of EC on the compressive strength of LWASCC is much weaker than that of *R* and EPS, as shown in Figure 5(b). Compared with *R*, EPS has a lower elastic modulus and weaker ITZs induced by its less rough surface. Therefore, LWASCC with EPS presents the poorest strength performance at a given volume fraction.

As mentioned above, SCC is a composite material with all the aggregates and microdefects suspended in the hydrated cement matrix. When exposed to dynamic loads, most of the vibration energy carried by vibration waves is dissipated at interfaces between aggregate/microdefect and the matrix, as shown in Figure 10(a). Therefore, the damping performance of SCC is significantly influenced by the aggregate type, ITZs, and pores. The different damping performances of LWASCC with three types of LWA are closely related to the intrinsic damping capacity of LWA and its bonding with the cement matrix. As illustrated in Figure 10(b), when exposed to dynamic loads, the introduction of EC with porous inner structure increases the reflection probability of vibration waves and thus dissipates more vibration energy. Therefore, the damping ratio of LWASCC with EC increases, as shown in Figure 9(a). It should be noted that the enhanced EC-matrix ITZs mitigates this tendency to some extent. Consequently, LWASCC with EC has a relatively lower increase rate of damping ratio at the same volume fraction (see Figure 9(b)), whereas, for LWASCC with *R* and EPS, as shown in Figures 10(b)–10(c) and Figures 11(b)–11(c), the poorly developed ITZs dissipate a large proportion of the vibration energy. In addition,

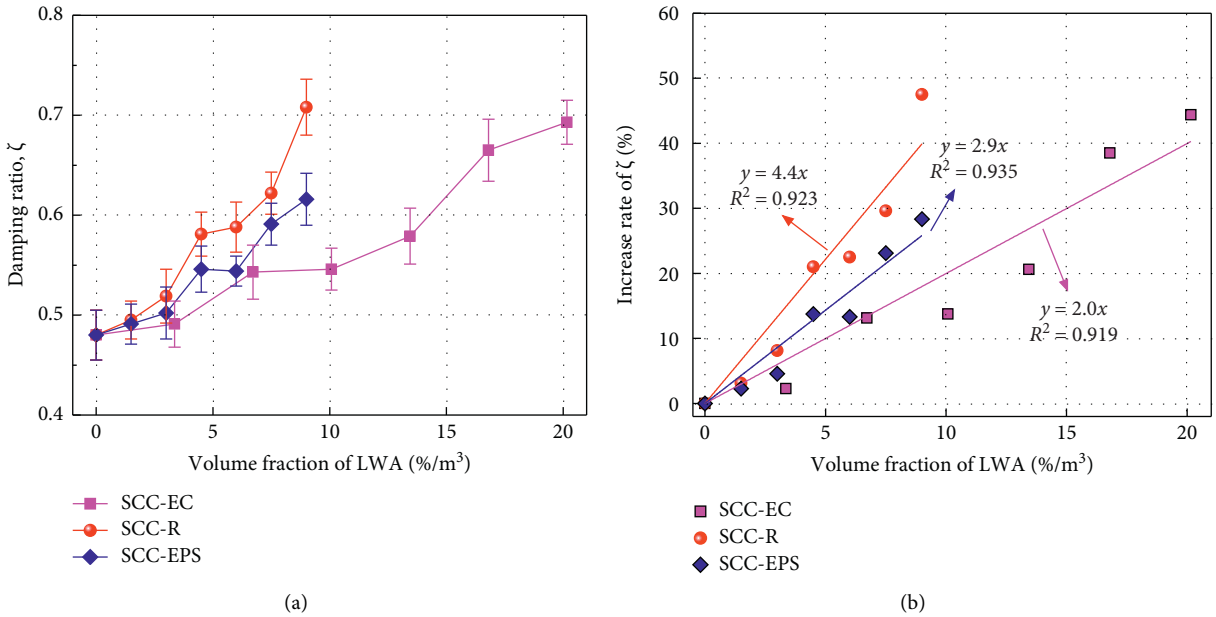

Figure 9: (a) Damping ratio and (b) its increase rate with LWAs.

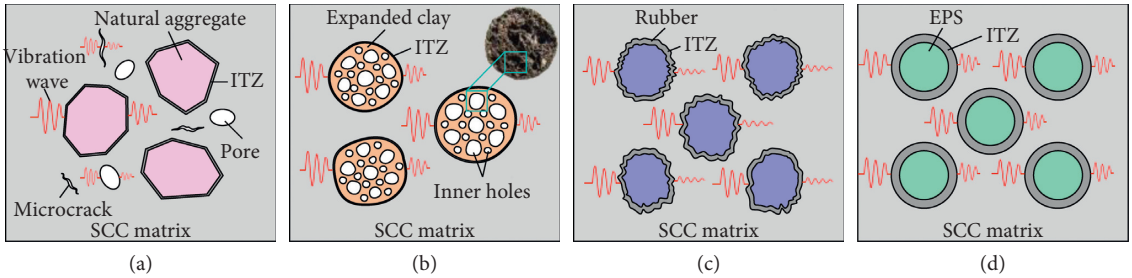

Figure 10: Schematic diagram of different aggregates in SCC. (a) Natural aggregate. (b) EC. (c) *R*. (d) EPS.

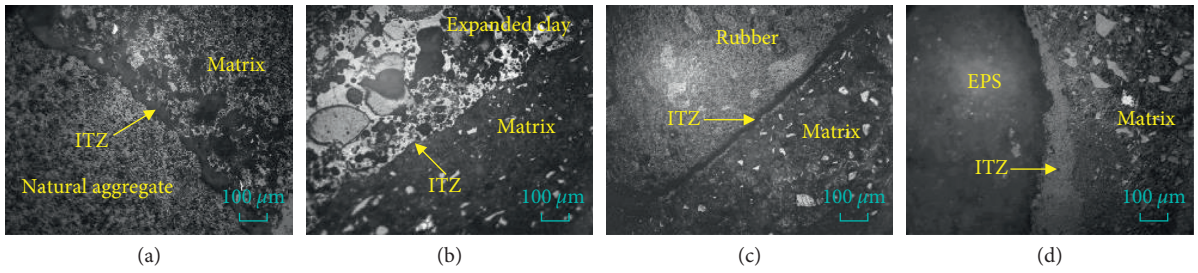

Figure 11: Micrographs of SCC with (a) natural aggregate, (b) EC, (c) *R*, and (d) EPS.

compared with EC, the relatively smaller sizes of *R* and EPS further increase the propagation path of vibration waves in LWAs, which dissipates more vibration energy. Especially for LWASCC with rubber, the excellent damping performance of rubber itself can consume a large proportion of the vibration energy [40, 41], as shown in Figure 10(c). Therefore, LWASCC with rubber shows the best damping performance of all the SCC series.

To sum up, the compressive strength and dynamic performances of LWASCC are highly influenced by the intrinsic properties (elastic modulus, damping capacity, wettability, etc.) and geometrical characteristics (size, surface roughness, etc.) of LWA, as well as the LWA-matrix bonding capacity. All the above factors should be carefully taken into consideration in developing LWASCC with adequate strength and outstanding dynamic performances.

5. Conclusions

(1) The addition of EC generally results in a slightly improved flowability of LWASCC and good passing ability with no visible blocking. However, the inclusion of *R* and EPS leads to a remarkable reduction in flowability of LWASCC and poor passing ability with minimal blocking.

(2) The inclusion of LWA leads to a decrease in compressive strength. The compressive strength reduction rate of LWASCC is 2.0%, 3.9%, and 4.0% by addition of 1% EC, *R*, and EPS in volume fraction, respectively.

(3) Both the dynamic elastic and shear modulus generally decreased with increasing LWA volume fraction. Incorporation of 1% volume of EC, *R*, and EPS reduced the dynamic elastic modulus of LWASCC by 1.83%, 1.61%, and 2.30%, respectively. The reduction rate of dynamic shear modulus is 1.88%, 1.51%, and 2.52% by addition of 1% EC, *R*, and EPS, respectively. The dynamic elastic and shear modulus show good linear dependence upon compressive strength.

(4) The addition of three types of LWA results in an amplitude of variation in dynamic Poisson's ratio no more than 10%, which indicates that the incorporation of LWA exerts limited influence on the transverse deformation capacity of LWASCC when subjected to dynamic loads.

(5) The damping ratio of LWASCC is improved by 2.0%, 4.4%, and 2.9% when the volume fraction of EC, *R*, and EPS is increased by 1%, respectively, indicating significantly enhanced energy dissipation capacity when subjected to dynamic loads. The different damping performances of LWASCC with three types of LWA are closely related to the intrinsic damping capacity of LWA and its bonding with cement paste.

(6) The compressive strength and dynamic performances of LWASCC are highly influenced by the intrinsic properties (elastic modulus, damping capacity, wettability, etc.) and geometrical characteristics (size, surface roughness, etc.) of LWA, as well as the LWA-matrix bonding capacity.

Data Availability

The data are not freely available due to third-party rights.

Conflicts of Interest

The authors declare that there are no conflicts of interest regarding the publication of this paper.

Acknowledgments

The authors would like to thank Dr. Hao Song and Dr. Wenxv Li of Central South University (CSU) for their great help in finishing the experimental work. This work was supported financially by the National Natural Science Foundation of China (Grants nos. 51678568 and 51905314).

References

[1] Z. Wu, Y. Zhang, J. Zheng, and Y. Ding, "An experimental study on the workability of self-compacting lightweight concrete," *Construction and Building Materials*, vol. 23, no. 5, pp. 2087–2092, 2009.

[2] S. C. Kou and C. S. Poon, "Properties of self-compacting concrete prepared with coarse and fine recycled concrete aggregates," *Cement and Concrete Composites*, vol. 31, no. 9, pp. 622–627, 2009.

[3] G. Long, Y. Gao, and Y. Xie, "Designing more sustainable and greener self-compacting concrete," *Construction and Building Materials*, vol. 84, pp. 301–306, 2015.

[4] K. Ma, J. Feng, G. Long, Y. Xie, and X. Chen, "Improved mix design method of self-compacting concrete based on coarse aggregate average diameter and slump flow," *Construction and Building Materials*, vol. 143, pp. 566–573, 2017.

[5] A. H. Nahhab and A. K. Ketab, "Influence of content and maximum size of light expanded clay aggregate on the fresh, strength, and durability properties of self-compacting lightweight concrete reinforced with micro steel fibers," *Construction and Building Materials*, vol. 233, p. 117922, 2020.

[6] J. Li, E. Zhao, J. Niu, and C. Wan, "Study on mixture design method and mechanical properties of steel fiber reinforced self-compacting lightweight aggregate concrete," *Construction and Building Materials*, vol. 267, p. 121019, 2021.

[7] J. Li, Y. Chen, and C. Wan, "A mix-design method for lightweight aggregate self-compacting concrete based on packing and mortar film thickness theories," *Construction and Building Materials*, vol. 157, pp. 621–634, 2017.

[8] Z. Yu, R. Tang, P. Cao, Q. Huang, X. Xie, and F. Shi, "Multiaxial test and failure criterion analysis on self-compacting lightweight aggregate concrete," *Construction and Building Materials*, vol. 215, pp. 786–798, 2019.

[9] J. Lv, T. Zhou, Q. Du, and K. Li, "Experimental and analytical study on uniaxial compressive fatigue behavior of self-compacting rubber lightweight aggregate concrete," *Construction and Building Materials*, vol. 237, p. 117623, 2020.

[10] Q. Fu, M. Bu, W. Xu et al., "Comparative analysis of dynamic constitutive response of hybrid fibre-reinforced concrete with different matrix strengths," *International Journal of Impact Engineering*, vol. 148, Article ID 103763, 2021.

[11] Q. Fu, W. Xu, D. Li et al., "Dynamic compressive behaviour of hybrid basalt-polypropylene fibre-reinforced concrete under confining pressure: experimental characterisation and strength criterion," *Cement and Concrete Composites*, vol. 118, Article ID 103954, 2021.

[12] B. H. AbdelAleem, M. K. Ismail, and A. A. A. Hassan, "The combined effect of crumb rubber and synthetic fibers on impact resistance of self-consolidating concrete," *Construction and Building Materials*, vol. 162, pp. 816–829, 2018.

[13] Y. Mohammadi, S. Mousavi, F. Rostami, and A. Danesh, "The effect of silica fume on the properties of self-compacted lightweight concrete," *Current World Environment*, vol. 10, no. 1, pp. 381–388, 2015.

[14] A. Lotfy, K. M. A. Hossain, and M. Lachemi, "Mix design and properties of lightweight self-consolidating concretes developed with furnace slag, expanded clay and expanded shale aggregates," *Journal of Sustainable Cement-Based Materials*, vol. 5, no. 5, pp. 297–323, 2015.

[15] D. S. L. Y. Wan, F. Aslani, and G. Ma, "Lightweight self-compacting concrete incorporating perlite, scoria, and polystyrene aggregates," *Journal of Materials in Civil Engineering*, vol. 30, no. 8, p. 04018178, 2018.

[16] İ. B. Topçu and T. Uygunoğlu, "Effect of aggregate type on properties of hardened self-consolidating lightweight concrete (SCLC)," *Construction and Building Materials*, vol. 24, no. 7, pp. 1286–1295, 2010.

[17] R. B. Ardalan, A. Joshaghani, and R. D. Hooton, "Workability retention and compressive strength of self-compacting concrete incorporating pumice powder and silica fume," *Construction and Building Materials*, vol. 134, pp. 116–122, 2017.

[18] M. Fathi, A. Yousefipour, and E. Hematpoury Farokhy, "Mechanical and physical properties of expanded polystyrene structural concretes containing micro-silica and nano-silica," *Construction and Building Materials*, vol. 136, pp. 590–597, 2017.

[19] A. A. A. Hassan, M. Lachemi, and K. M. A. Hossain, "Effect of metakaolin and silica fume on rheology of self-consolidating concrete," *Cement and Concrete Composites*, vol. 34, no. 6, pp. 801–807, 2012.

[20] B. H. AbdelAleem and A. A. A. Hassan, "Development of self-consolidating rubberized concrete incorporating silica fume," *Construction and Building Materials*, vol. 161, pp. 389–397, 2018.

[21] K. B. Najim and M. R. Hall, "A review of the fresh/hardened properties and applications for plain-(PRC) and self-compacting rubberised concrete (SCRC)," *Construction and Building Materials*, vol. 24, no. 11, pp. 2043–2051, 2010.

[22] G. C. Long, K. L. Ma, X. Xie et al., "Effect of RA on reduction of compressive strength of concrete," *Journal of Building Materials*, vol. 16, no. 5, pp. 758–762, 2013, in Chinese.

[23] Q. Fu, M. Bu, W. Xu et al., "Comparative analysis of dynamic constitutive response of hybrid fibre-reinforced concrete with different matrix strengths," *International Journal of Impact Engineering*, vol. 148, p. 103763, 2021.

[24] L. Zheng, X. Sharon Huo, and Y. Yuan, "Experimental investigation on dynamic properties of rubberized concrete," *Construction and Building Materials*, vol. 22, no. 5, pp. 939–947, 2008.

[25] I. M. Nikbin and M. Golshekan, "The effect of expanded polystyrene synthetic particles on the fracture parameters, brittleness and mechanical properties of concrete," *Theoretical and Applied Fracture Mechanics*, vol. 94, pp. 160–172, 2018.

[26] G. Long, J. Yang, and Y. Xie, "The mechanical characteristics of steam-cured high strength concrete incorporating with lightweight aggregate," *Construction and Building Materials*, vol. 136, pp. 456–464, 2017.

[27] P. Tang and H. J. H. Brouwers, "The durability and environmental properties of self-compacting concrete incorporating cold bonded lightweight aggregates produced from combined industrial solid wastes," *Construction and Building Materials*, vol. 167, pp. 271–285, 2018.

[28] M. Kurt, M. S. Gül, R. Gül, A. C. Aydin, and T. Kotan, "The effect of pumice powder on the self-compactability of pumice aggregate lightweight concrete," *Construction and Building Materials*, vol. 103, pp. 36–46, 2016.

[29] E. Güneyisi, M. Gesoglu, O. A. Azez, and H. Ö. Öz, "Effect of nano silica on the workability of self-compacting concretes having untreated and surface treated lightweight aggregates," *Construction and Building Materials*, vol. 115, pp. 371–380, 2016.

[30] M. I. Kaffetzakis and C. G. Papanicolaou, "Bond behavior of reinforcement in lightweight aggregate self-compacting concrete," *Construction and Building Materials*, vol. 113, pp. 641–652, 2016.

[31] ASTM C 1611, *Standard Test Method for Slump Flow of Self-Consolidating Concrete*, ASTM C 1611, West Conshohocken, PA, USA, 2014.

[32] ASTM C 1621, *Standard Test Method for Passing Ability of Self-Consolidating Concrete by J-Ring*, ASTM C 1621, West Conshohocken, PA, USA, 2009.

[33] GB/T 50081, *Standard for Test Method of Mechanical Properties on Ordinary Concrete*, GB/T 50081, Beijing, China, 2002.

[34] ASTM C 215, *Standard Test Method for Fundamental Transverse, Longitudinal, and Torsional Resonant Frequencies of Concrete Specimens*, ASTM C 215, West Conshohocken, PA, USA, 2014.

[35] S. Guo, Q. Dai, R. Si, X. Sun, and C. Lu, "Evaluation of properties and performance of rubber-modified concrete for recycling of waste scrap tire," *Journal of Cleaner Production*, vol. 148, pp. 681–689, 2017.

[36] M. M. R. Taha, A. S. El-Dieb, M. A. A. El-Wahab, and M. E. Abdel-Hameed, "Mechanical, fracture, and microstructural investigations of rubber concrete," *Journal of Materials in Civil Engineering*, vol. 20, no. 10, pp. 640–649, 2008.

[37] K. B. Najim and M. R. Hall, "Mechanical and dynamic properties of self-compacting crumb rubber modified concrete," *Construction and Building Materials*, vol. 27, no. 1, pp. 521–530, 2012.

[38] N. Li, G. Long, Q. Fu, X. Wang, K. Ma, and Y. Xie, "Effects of freeze and cyclic flexural load on mechanical evolution of filling layer self-compacting concrete," *Construction and Building Materials*, vol. 200, pp. 198–208, 2019.

[39] A. Dall'Asta and L. Ragni, "Experimental tests and analytical model of high damping rubber dissipating devices," *Engineering Structures*, vol. 28, no. 13, pp. 1874–1884, 2006.

[40] X.-Y. Zhao, P. Xiang, M. Tian, H. Fong, R. Jin, and L.-Q. Zhang, "Nitrile butadiene rubber/hindered phenol nanocomposites with improved strength and high damping performance," *Polymer*, vol. 48, no. 20, pp. 6056–6063, 2007.

[41] A. F. M. S. Amin, A. Lion, S. Sekita, and Y. Okui, "Nonlinear dependence of viscosity in modeling the rate-dependent response of natural and high damping rubbers in compression and shear: experimental identification and numerical verification," *International Journal of Plasticity*, vol. 22, no. 9, pp. 1610–1657, 2006.